SUPPORTING INFORMATION

X‑ray-Induced Shortwave Infrared Biomedical Imaging Using Rare-Earth Nanoprobes

Dominik Jan Naczynski,[†] Conroy Sun,[†] Silvan Türkcan,[†] Cesare Jenkins,[†,‡] Ai Leen Koh,[§] Debra Ikeda,[‖] 4 Guillem Pratx,[†] and Lei Xing[*,†]

[†] Department of Radiation Oncology, Stanford University School of Medicine, Palo Alto, California 94305

[‡] Department of Mechanical Engineering, Stanford University, Palo Alto, California 94305

[§] Stanford Nanocharacterization Laboratory, Stanford University, Palo Alto, California 94305

[‖] Department of Radiology, Stanford University School of Medicine, Palo Alto, California 94305

[*]To whom correspondences should be addressed: lei@stanford.edu

Materials and Methods

Synthesis of rare earth nanoparticles

$NaYF_4$: Er, Yb nanoparticles were prepared using a well-established solvothermal decomposition method[1]. Briefly, rare earth trifluoroacetate precursors were dissolved in oleylamine. The shell precursor solution was prepared by dissolving stoichiometric amounts of the sodium and yttrium trifluoroacetates in oleylamine. The core solution was then heated to 340°C under vigorous stirring in inert nitrogen atmosphere to allow the formation of the core. Next, the shell precursor was added and after cooling, the synthesized nanoparticles were precipitated out of solution and washed repeatedly with ethanol. The resulting REs were surface modified with DSPE–2000-PEG by ligand exchange performed in tetrahydrofuran (THF) under ultrasonication (Branson Ultrasonic Corp.). The PEGylated REs were then added dropwise into deionized water and excess THF was evaporated overnight under gentle heating (40°C). Any remaining aggregates were removed by a 0.22 μm filter.

Nanoparticle characterization

As-synthesized REs were visualized by transmission electron microscopy (TEM). TEM specimens were prepared by depositing a drop of diluted nanoparticle suspension on copper grids coated with ultrathin carbon support film (Ted Pella). TEM images were acquired using an FEI 80-300 Titan operating at 300 kV. Hydrodynamic size was measured in PBS using Zetasizer Nano series dynamic light scattering (DLS) particle size analyzer (Malvern Instruments). Emission spectra of REs were collected from a dried pellet (~0.5 g) of nanoparticles following exposure to either X-rays generated from a mini X-ray source (Ampex) or NIR light generated

from a 975 nm laser diode (B&W Tek). Spectra was collected using a spectrometer (Princeton Instruments) coupled to an InGaAs detector.

X-IR imaging system

X-ray induced SWIR emissions were visualized using a custom built imaging system. The system consisted of an X-ray source (X-RAD 320, PXi Precision X-ray) positioned approximately 45 cm above the sample being imaged and an InGaAs camera (NIRvana 640, Princeton Instruments) perpendicular to the source. The camera was placed directly behind a shielded glass window approximately 12 in away from the sample. Black curtains were used to darken the imaging space. Acquired X-IR images were processed using ImageJ.

***In vivo* X-IR Imaging**

All animal studies were conducted in accordance with Stanford University Institutional Animal Care and Use Committee (IACUC) approved protocols. For SNR studies, nude mice were subcutaneously injected with a mixture of matrigel and 0.1 or 1.0 mg of PEGylated REs into the back flank. For biodistribution imaging, nude mice were intravenously injected with approximately 100 μl of 5 mg/ml PEGylated REs via the tail vein and imaged after 15 minutes using the X-IR system operating at 320 kVp and 12.5 mA. In the lymphatic mapping studies, we subcutaneously administered approximately 10 μl of a 20 mg/ml solution of PEGylated REs in the forepaw of nude mice and imaged nanoparticle drainage over 15 minutes. All mice were anesthetized with an intraperitoneal injection of a ketamine hydrochloride and xylazine cocktail prior to imaging.

Supporting Figures

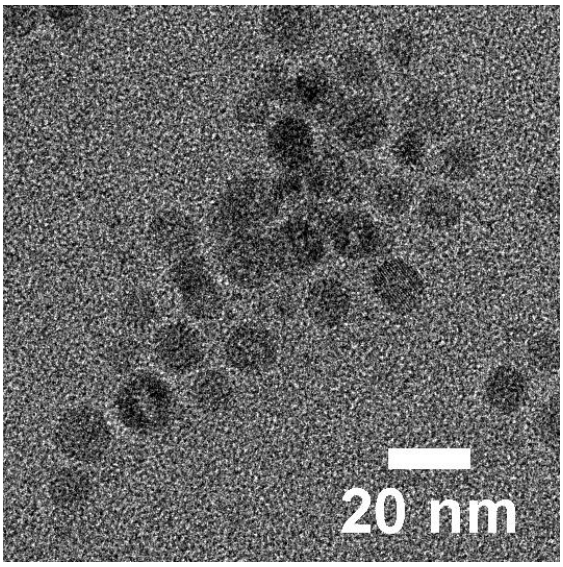

Figure S1. TEM images of "core" only REs ($NaYF_4$:Er, Yb) reveals monodispersed nanoparticles with spherical morphology.

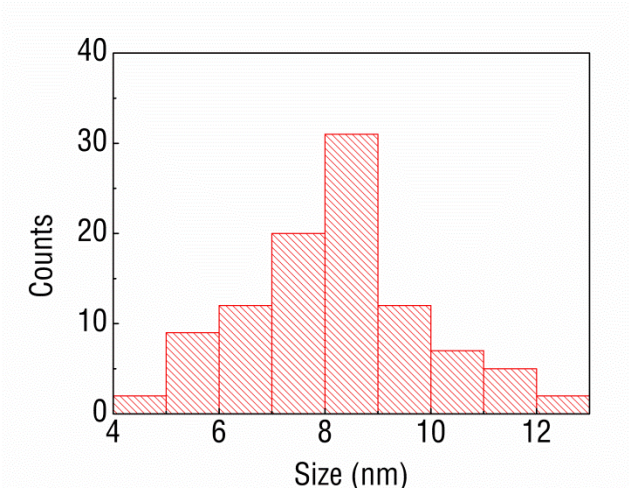

Figure S2. Size distribution of "core" only REs shows a narrow population of nanoparticles notably smaller than their core-shell counterparts.

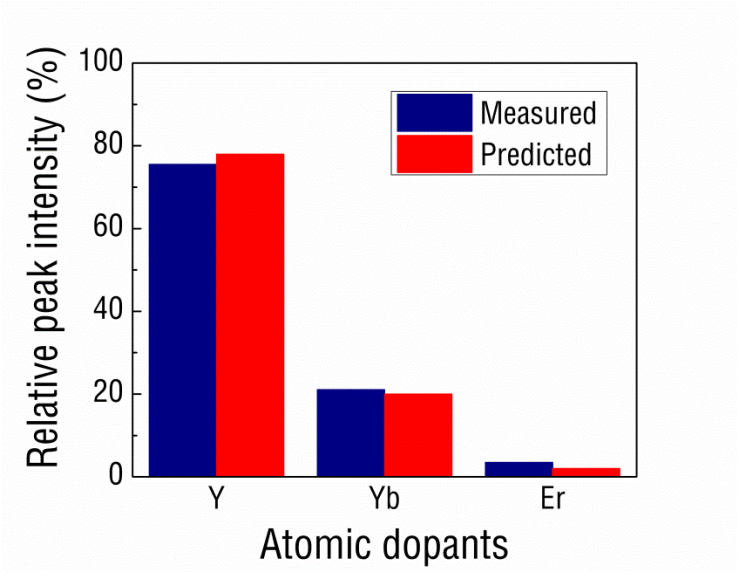

Figure S3 – Relative EDS peak intensities of rare-earth dopants in $NaYF_4$: 2% Er, 20% Yb nanoparticles (REs) compared to predicted values.

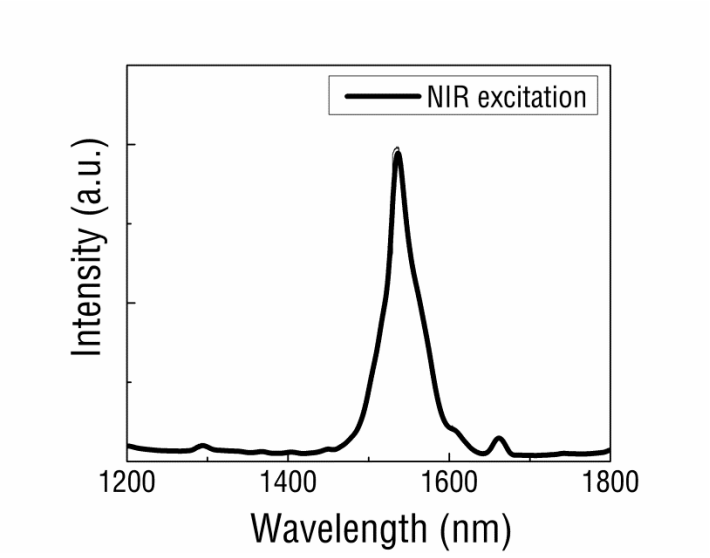

Figure S4 - In addition to X-ray induced SWIR emission, REs display intense SWIR emissions when excited with NIR light (980 nm).

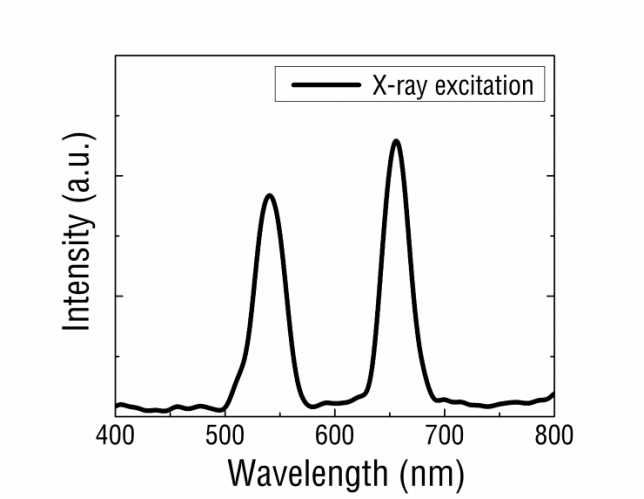

Figure S5 - X-ray excitation also induced visible emissions, similar to the observed upconversion fluorescence emissions after NIR excitation.

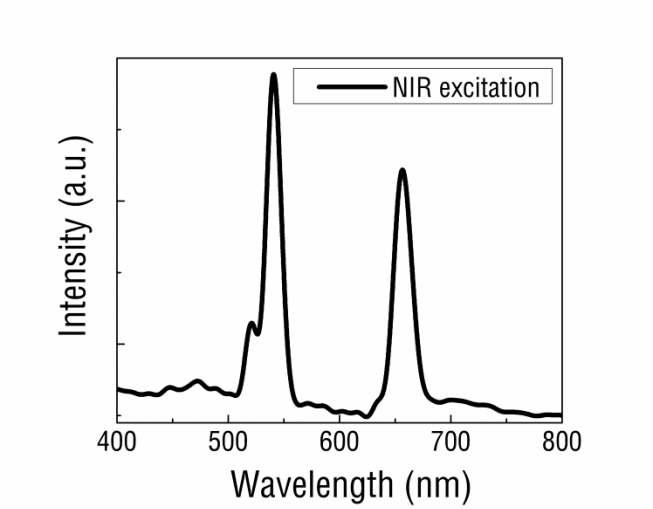

Figure S6 – REs also display upconversion fluorescence through NIR excitation to generate visible emissions at 540 and 650 nm.

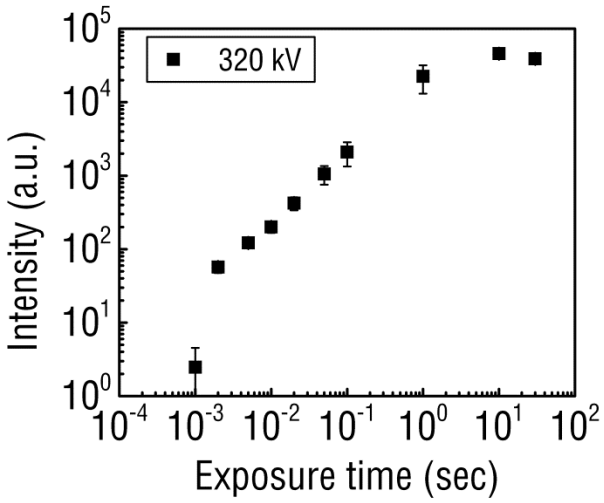

Figure S7. Exposure sensitivity of the X-IR imaging system was assessed by exciting $NaYF_4$: Er,Yb REs under 320 kVp X-rays.

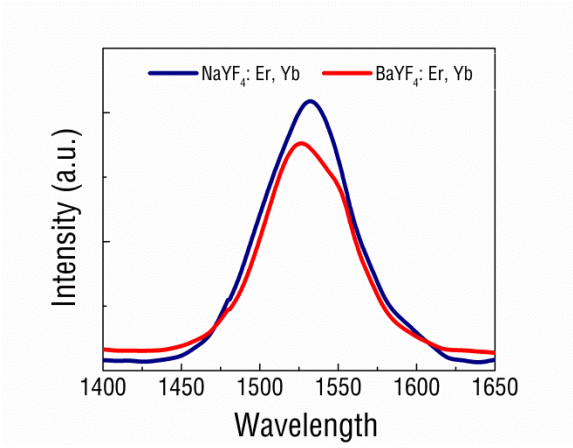

Figure S8. X-IR spectrum of $BaYF_4$: Er,Yb and $NaYF_4$: Er,Yb REs show distinct SWIR emission peaks centered around 1530 nm after X-ray irradiation.

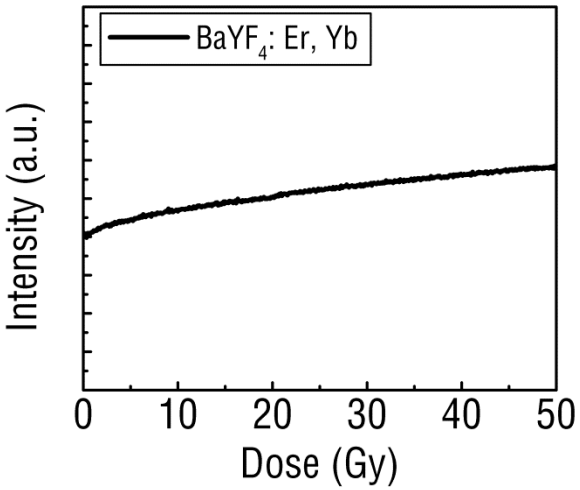

Figure S9. $BaYF_4$: Er,Yb REs retain SWIR emission intensity after extended exposure to high energy (320 kVp) X-rays.

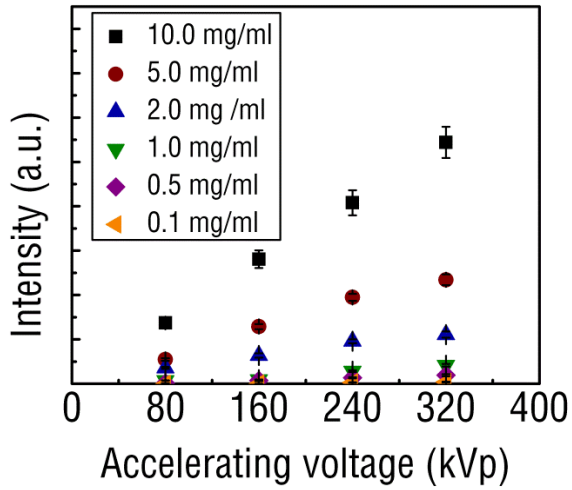

Figure S10. The X-IR detection sensitivity of $BaYF_4$: Er,Yb REs was measured as a function of X-ray accelerating voltage. Error bars represent pixel-to-pixel variation within a region of interest and propagated over three samples.

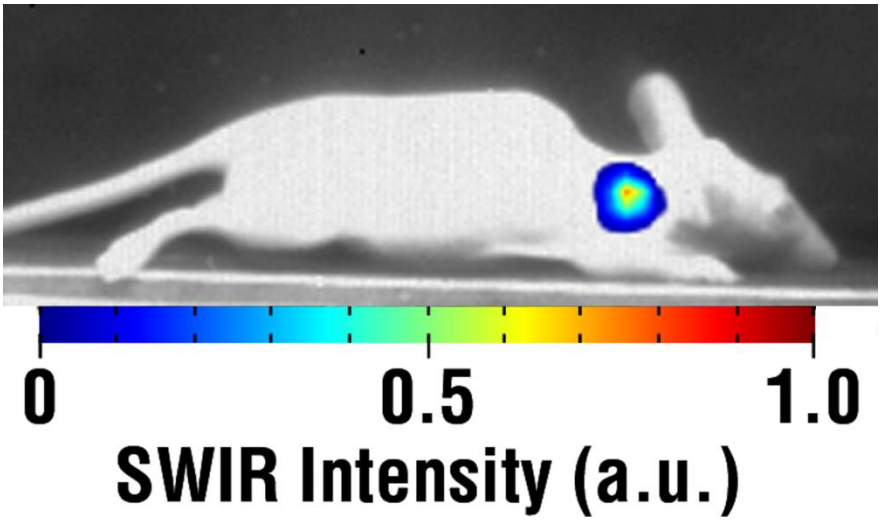

Figure S11. X-IR imaging of approximately 1 mg of $BaYF_4$: Er, Yb nanoparticles injected subcutaneously in a nude mouse. Imaging performed using 320 kVp X-rays under 10 s exposure.

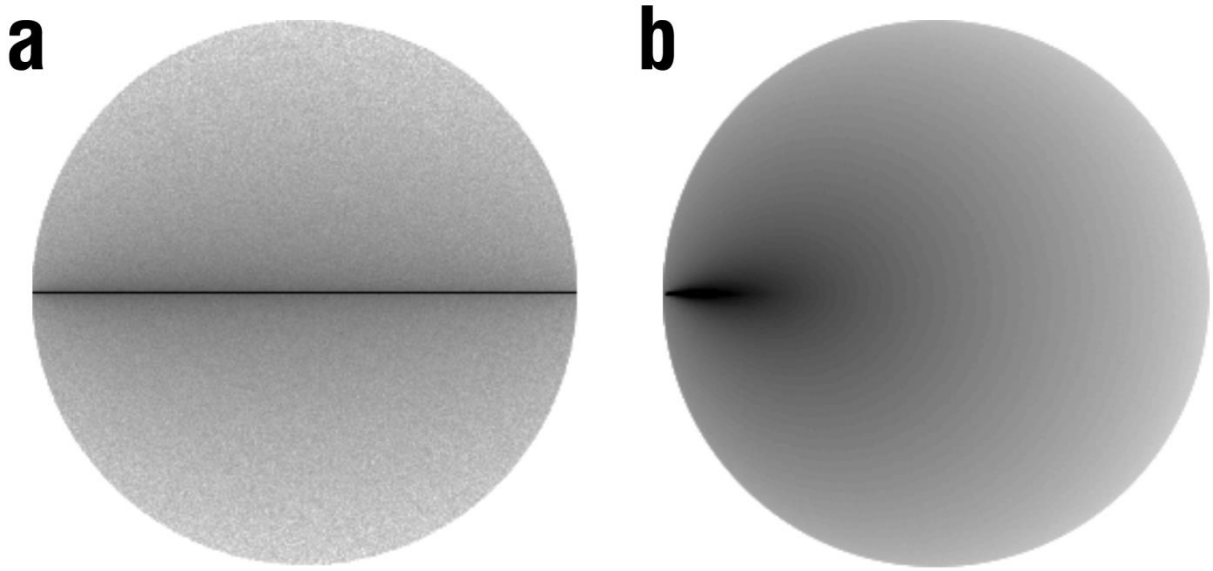

Figure S12. (A) Propagation of a NIR laser beam (λ=800 nm) through a 5 mm-diameter tissue phantom (Monte Carlo simulation; μ_a = 0.0025 cm^{-1}, μ_s = 7.8 cm^{-1}, and n=1.3). (B) Propagation

of a monochromatic X-ray beam (100 keV) through a water phantom of the same size (Monte Carlo simulation). Both images are on a log scale.

1. Naczynski, D. J.; Tan, M. C.; Zevon, M.; Wall, B.; Kohl, J.; Kulesa, A.; Chen, S.; Roth, C. M.; Riman, R. E.; Moghe, P. V. *Nat. Commun.* **2013,** 4, 2199.